

# TIME DOMAIN COMPARISONS OF MEASURED AND SPECTRALLY SIMULATED BREAKING WAVES

Mustafa Kemal Özalp<sup>1</sup> and Serdar Beji<sup>1</sup>

For realistic wave simulations in the nearshore zone besides nonlinear interactions the dissipative effects of wave breaking must also be taken into account. This paper presents the applications of a spectral nonlinear wave model with a dissipative breaking mechanism introduced by Beji and Nadaoka (1997). Results obtained for spectral components are converted to the time series and compared with Beji and Battjes' (1993) laboratory measurements and the field measurements of Nakamura and Katoh (1992) in the surf zone. While the model predicts the spilling-type breaking of irregular waves in acceptable agreement with the measurements in time domain, the agreement is unsatisfactory for plunging-type breakers.

*Keywords: Spectral model; wave breaking; numerical simulation*

## INTRODUCTION

Waves play active role in the formation of coastal lines, sediment transport and are important in the design of coastal and offshore structures. For realistic wave simulations in the nearshore zone besides nonlinear interactions the dissipative effects of wave breaking must also be taken into account.

There are different methods used to model the wave breaking phenomena. An accurate but time consuming approach is the numerical solution of Navier-Stokes Equations (NSE), such as DNS, LES and RANS. On the other hand, concepts using the nonlinear shallow water equations or the Boussinesq equations are computationally very efficient; such as surface roller introduced by Svendsen (1984a, b) and “artificial eddy viscosity term” which was proposed by J.A. Zelt (1991). A different technique of introducing wave breaking into wave models as a dissipation term is suggested by Battjes and Janssen (1978) and Battjes (1986). Eldeberky & Battjes (1996) and Beji & Nadaoka (1997) further implemented the proposed dissipation terms into spectral wave models.

This paper presents the applications of a spectral nonlinear wave model with a dissipative breaking mechanism (Beji and Nadaoka, 1997). Results obtained for spectral components are converted to time series. Numerical results both in spectral and time domain were later compared with the laboratory experiments (Beji and Battjes, 1993) and field observations (Nakamura and Katoh, 1992). Comparisons in spectral domain shows quite acceptable agreements. While the model predicts the spilling-type breaking of irregular waves in acceptable agreement with the measurements in time domain, the agreement is unsatisfactory for plunging-type breakers. There is a small phase shift occurring in simulations of both cases. While this problem may be related to the numerical algorithm, deviations in the wave profile between the predictions and experiments suggest the necessity for an improvement in the dissipation term.

## EVOLUTION EQUATIONS

A nonlinear spectral model valid for arbitrary water depths (Beji and Nadaoka, 1999) is used to model wave propagation over arbitrary depths

$$\begin{aligned} \frac{da_n}{dx} = & -\frac{a_s}{a_1} a_n + \beta \sum_{m=1}^{N-n} a^+ [(a_m b_{n+m} - a_{n+m} b_m) \cos \theta^+ + (a_m a_{n+m} + b_m b_{n+m}) \sin \theta^+] \\ & + \frac{1}{2} \beta \sum_{m=1}^{n-1} a^- [(a_m b_{n-m} + a_{n-m} b_m) \cos \theta^- + (a_m a_{n-m} - b_m b_{n-m}) \sin \theta^-] \end{aligned} \quad (1a)$$

---

<sup>1</sup> Faculty of Naval Architecture and Ocean Engineering, Istanbul Technical University, Maslak 34469, Istanbul, Turkey

$$\frac{db_n}{dx} = -\frac{a_s}{a_1}b_n - \beta \sum_{m=1}^{N-n} a^+ [(a_m a_{n+m} + b_m b_{n+m}) \cos \theta^+ - (a_m b_{n+m} - b_{n+m} b_m) \sin \theta^+] + \frac{1}{2} \beta \sum_{m=1}^{n-1} a^- [(a_m a_{n-m} + b_m b_{n-m}) \cos \theta^- - (a_m b_{n-m} + a_{n-m} b_m) \sin \theta^-] \quad (1b)$$

where  $N$  is the number of frequency components retained in the solution, and

$$a^+ = \frac{k_{n+m} - k_m}{a_1 + a_2 \delta^+}, \quad a^- = \frac{k_{n-m} + k_m}{a_1 + a_2 \delta^-},$$

$$\delta^+ = k_{n+m} - k_m - k_n, \quad \delta^- = k_{n-m} + k_m - k_n,$$

$$\theta^+ = \int_0^x (k_{n+m} - k_m - k_n) dx, \quad \theta^- = \int_0^x (k_{n-m} + k_m - k_n) dx \quad (2)$$

$$a_s = \frac{1}{2} [C_p (C_g)_x + (C_p - C_g) (C_p)_x] + \frac{(C_p - C_g)}{k^2} \left( \frac{3}{2} C_p k_n - \omega_n \right) (k_n)_x$$

$$a_1 = \frac{1}{2} C_p (C_p - C_g) - 2 \frac{(C_p - C_g)}{k^2} \omega_n k_n + \frac{3 C_p (C_p - C_g)}{2 k^2} k_n^2, \quad \beta = \frac{3}{4} g \left( 3 - 2 \frac{C_g}{C_p} - \frac{k^2 C_p^4}{g^2} \right)$$

where  $\omega_n$  is the radian frequency which is equal to  $n\Delta\omega$ ,  $\Delta\omega$  being the frequency resolution.  $k_n$  is computed for each component from the linear dispersion relation of the wave model for the local depth  $h(x)$ :

$$C_g \omega_n - \frac{1}{2} C_p (C_p + C_g) k_n + \frac{(C_p - C_g)}{k^2} \omega_n k_n^2 - \frac{C_p (C_p - C_g)}{2 k^2} k_n^3 = 0 \quad (3)$$

Eq. (1a) and (1b) are semi-empirically modified so as to include wave breaking effects as in Beji and Nadaoka (1997). The breaking modification is introduced in the same vein as Battjes' (1986) dissipation model for periodic waves. Thus, breaking effects in the spectral evolution equations are modelled as

$$\left( \frac{da_n}{dx} \right)_d = -\frac{B}{2\pi\gamma^3} \frac{\omega_n}{(C_g)_n} \left( \frac{2gH}{C_p^2} \right)^4 a_n \quad (4)$$

$$\left( \frac{db_n}{dx} \right)_d = -\frac{B}{2\pi\gamma^3} \frac{\omega_n}{(C_g)_n} \left( \frac{2gH}{C_p^2} \right)^4 b_n$$

where  $a_n$ 's and  $b_n$ 's are the spatially evolving Fourier amplitudes of the spectral model,  $C_p$  is the local phase celerity computed for the dominant wave frequency  $\omega$  and local depth  $h$ .  $(C_g)_n$  denotes the group velocity corresponding to the frequency  $\omega_n$  and local depth  $h$  according to the linear theory. The free index  $n$  runs from 1 to  $N$ , resulting in  $2N$  number of nonlinearly coupled first-order differential equations for the unknown components  $a_n(x)$  and  $b_n(x)$ .

The final form of the breaking wave model is formed by adding the expressions in eq. (3) to the right-hand sides of (1a) and (1b):

$$\begin{aligned} \frac{da_n}{dx} = & -\frac{a_s}{a_1} a_n + \beta \sum_{m=1}^{N-n} a^+ [(a_m b_{n+m} - a_{n+m} b_m) \cos \theta^+ + (a_m a_{n+m} + b_m b_{n+m}) \sin \theta^+] \\ & + \frac{1}{2} \beta \sum_{m=1}^{n-1} a^- [(a_m b_{n-m} + a_{n-m} b_m) \cos \theta^- + (a_m a_{n-m} - b_m b_{n-m}) \sin \theta^-] \\ & - \frac{B}{2\pi\gamma^3} \frac{\omega_n}{(C_g)_n} \left(\frac{2gH}{C_p^2}\right)^4 a_n - \frac{B}{2\pi\gamma^3} \frac{\omega_n}{(C_g)_n} \left(\frac{2gH}{C_p^2}\right)^4 b_n \end{aligned} \quad (5a)$$

$$\begin{aligned} \frac{db_n}{dx} = & -\frac{a_s}{a_1} b_n - \beta \sum_{m=1}^{N-n} a^+ [(a_m a_{n+m} + b_m b_{n+m}) \cos \theta^+ - (a_m b_{n+m} - b_{n+m} b_m) \sin \theta^+] \\ & + \frac{1}{2} \beta \sum_{m=1}^{n-1} a^- [(a_m a_{n-m} + b_m b_{n-m}) \cos \theta^- - (a_m b_{n-m} + a_{n-m} b_m) \sin \theta^-] \\ & - \frac{B}{2\pi\gamma^3} \frac{\omega_n}{(C_g)_n} \left(\frac{2gH}{C_p^2}\right)^4 a_n - \frac{B}{2\pi\gamma^3} \frac{\omega_n}{(C_g)_n} \left(\frac{2gH}{C_p^2}\right)^4 b_n \end{aligned} \quad (5b)$$

## NUMERICAL SIMULATIONS

The modified spectral model is used for simulations of experiments of breaking waves over a bar and of actual breaking waves in the surf zone. Then the spectral output of the wave model is converted to the time domain and both spectral and time domain numerical results are compared with the actual data.

Beji and Battjes' (1993) experimental measurements for waves with a JONSWAP type wave spectrum is simulated first. The peak frequency  $f_p$  is 0.4 Hz for long waves and 1.0 Hz for short waves. The dominant frequency for the wave model is assigned to the mean frequency of the incident wave spectrum. Surface elevation data gathered at station 1 was segmented into 6 portions with 4096 data points and each portion was Fourier transformed. As a result, 2048 pairs of Fourier components, which covered a frequency range of 0.0024 – 5.0018 Hz, are calculated for each segment and used to reproduce the incident wave spectrum. The spectra are obtained after ensemble averaging all the realizations and frequency smoothing 40 neighbouring components. Finally, the Fourier coefficients of the spectra are used to compute time domain results at each station via Inverse Fourier Transform. This process is repeated for six different cases, half of them being non-breaking, spilling, and plunging-type breaking long waves and the other half being short waves with each type of breaker indicated.

Next, the model is used to simulate the field measurements of Nakamura and Katoh (1992) on February 28. Stations 1-7 were located in the surf zone and hence the breaking effects were dominant over these stations. Stations 3-7 are used for numerical simulations since station 1 and 2 are virtually in the swash zone. The peak frequency for random waves is 0.078 Hz which corresponds to the period of 12.8 s. The numerical procedure used is the same as the experimental case. Surface elevation data at the Station 7 is divided into 12 portions with 1024 data points each and then Fourier transformed. 400 of the resultant 512 pairs of Fourier components, which covered a frequency range of 0.0020 – 0.7812 Hz, are used to generate the incident wave spectrum. Frequency smoothing was performed for 16 neighbouring components.

## RESULTS

Comparisons are given under separate headings. Figures show the spectral and time domain comparisons of measured and simulated waves.

### Breaking and non-breaking random waves over a submerged bar

Spectral and time domain comparisons of numerical simulations and experimental data of Beji and Battjes (1993) are given first for short and then for long waves. There are 8 stations both in numerical simulations and experimental measurements. Spectral and time domain comparisons are presented side by side for ease of comparing. Figure 1, 2, and 3 show spectral and time domain comparisons for short non-breaking and breaking waves.

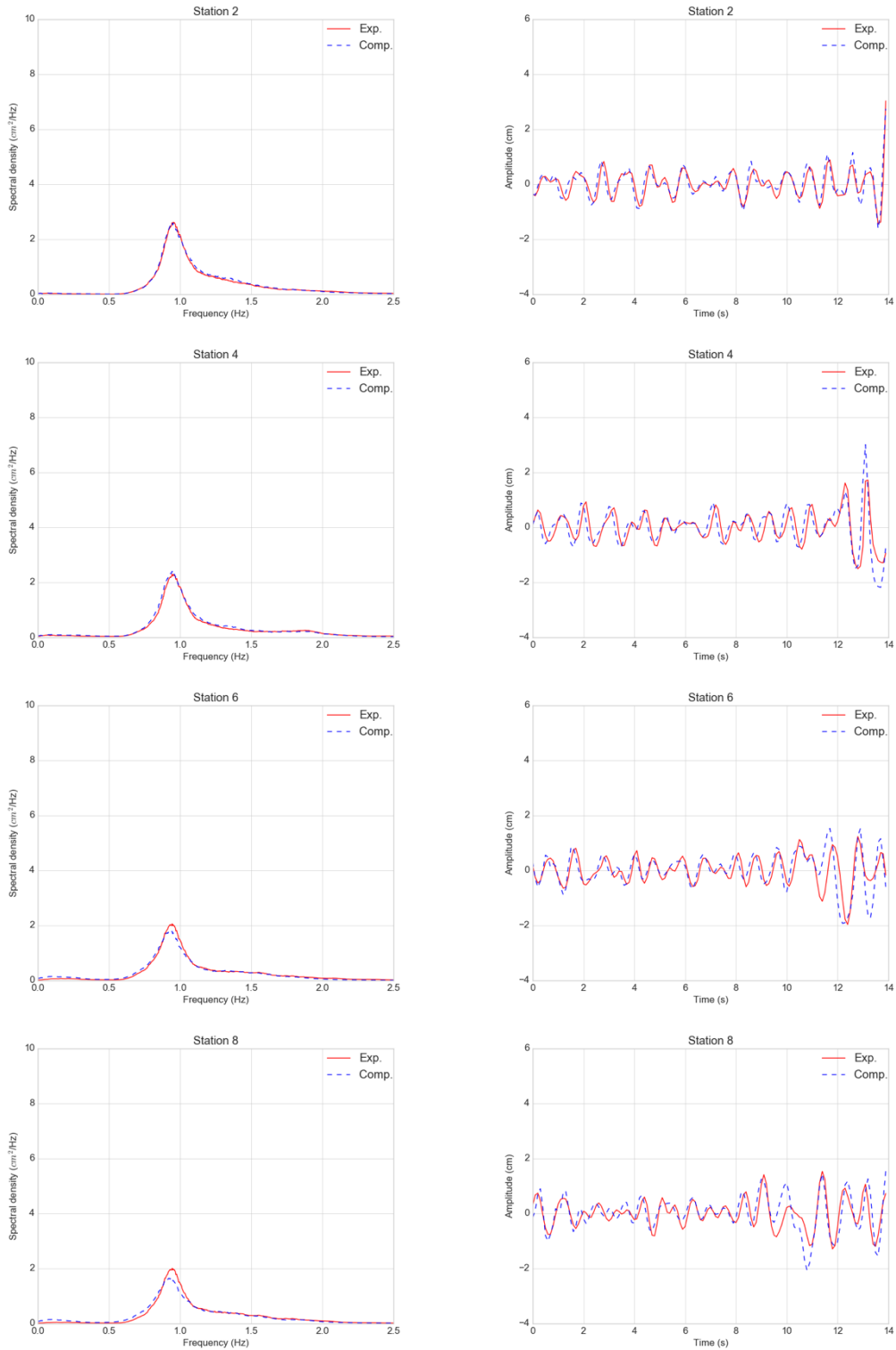


Figure 1. Random non-breaking short waves with  $f_p = 1.0$  Hz over a submerged bar. Left column shows wave spectra, right column shows time domain series. Solid line: experimental measurements, dashed line: computational results.

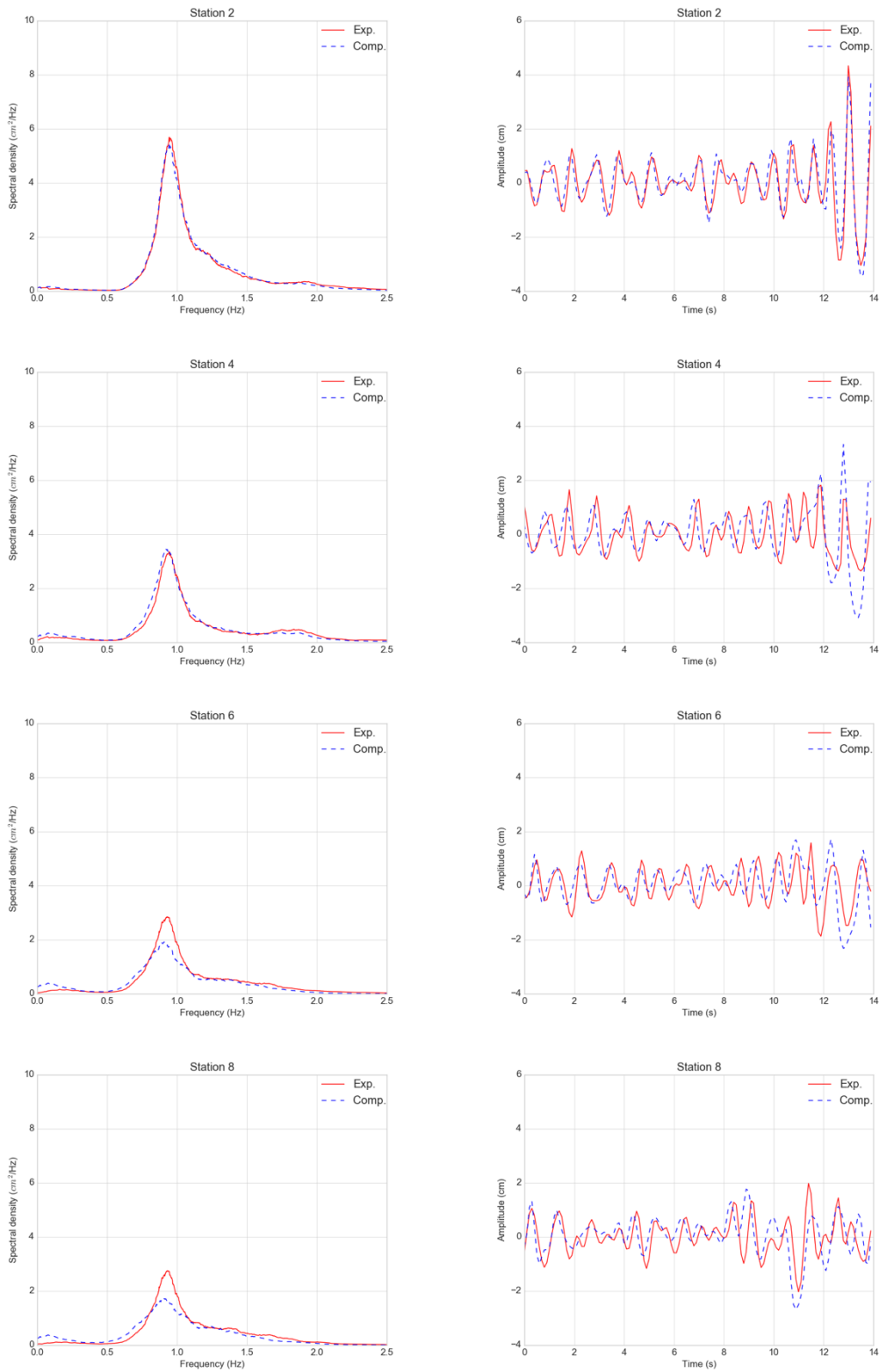
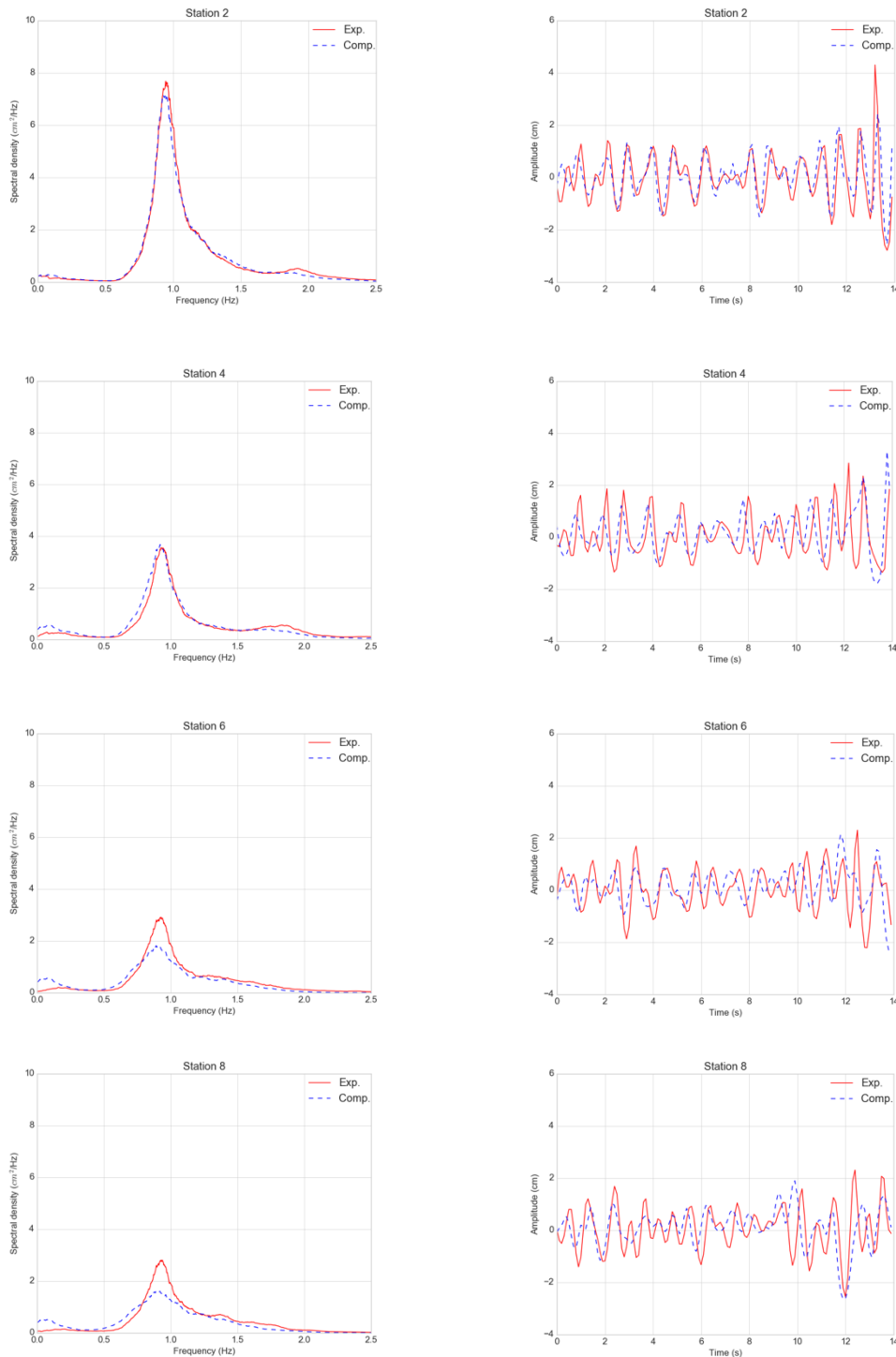


Figure 2. Random spilling-type breaking short waves with  $f_p = 1.0$  Hz over a submerged bar. Left column shows wave spectra, right column shows time domain series. Solid line: experimental measurements, dashed line: computational results.



**Figure 3. Random plunging-type breaking short waves with  $f_p = 1.0$  Hz over a submerged bar. Left column shows wave spectra, right column shows time domain series. Solid line: experimental measurements, dashed line: computational results.**

Although spectral domain results for random non-breaking and breaking short waves show good overall agreement, computations deviate once the waves start breaking. Likewise, the time domain results are good for the first few stations, but the deviations grow for the latter stations. In addition, a small phase shift exists in each time domain computation.

Figures 4, 5, and 6 belong to non-breaking and breaking random long waves. In this case, the spectral domain results show better agreement in comparison to short waves. The agreement in time domain results are better for non-breaking long waves. However, computations start deviating after the waves begin breaking.

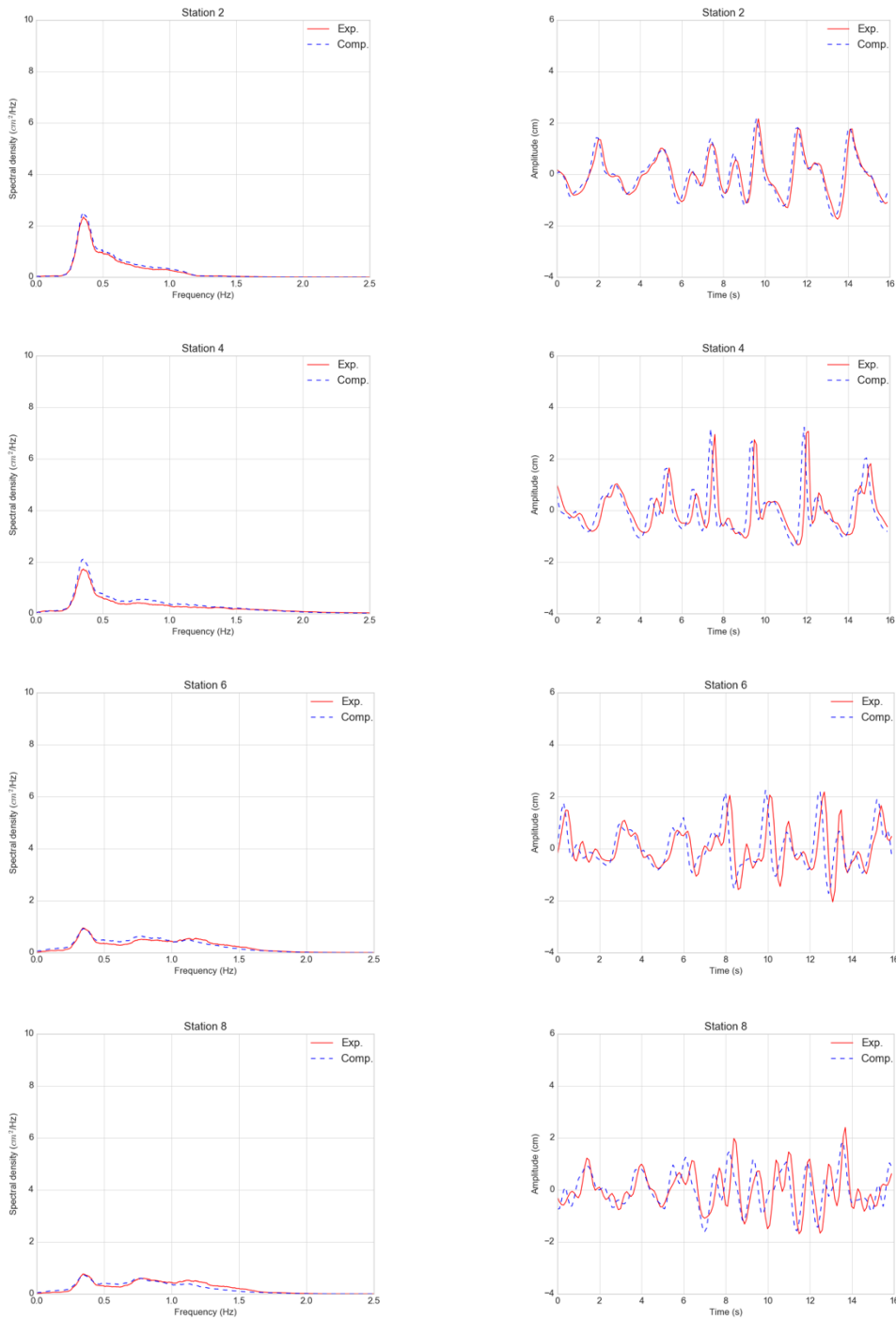


Figure 4. Random non-breaking long waves with  $f_p = 0.4 \text{ Hz}$  over a submerged bar. Left column shows wave spectra, right column shows time domain series. Solid line: experimental measurements, dashed line: computational results.

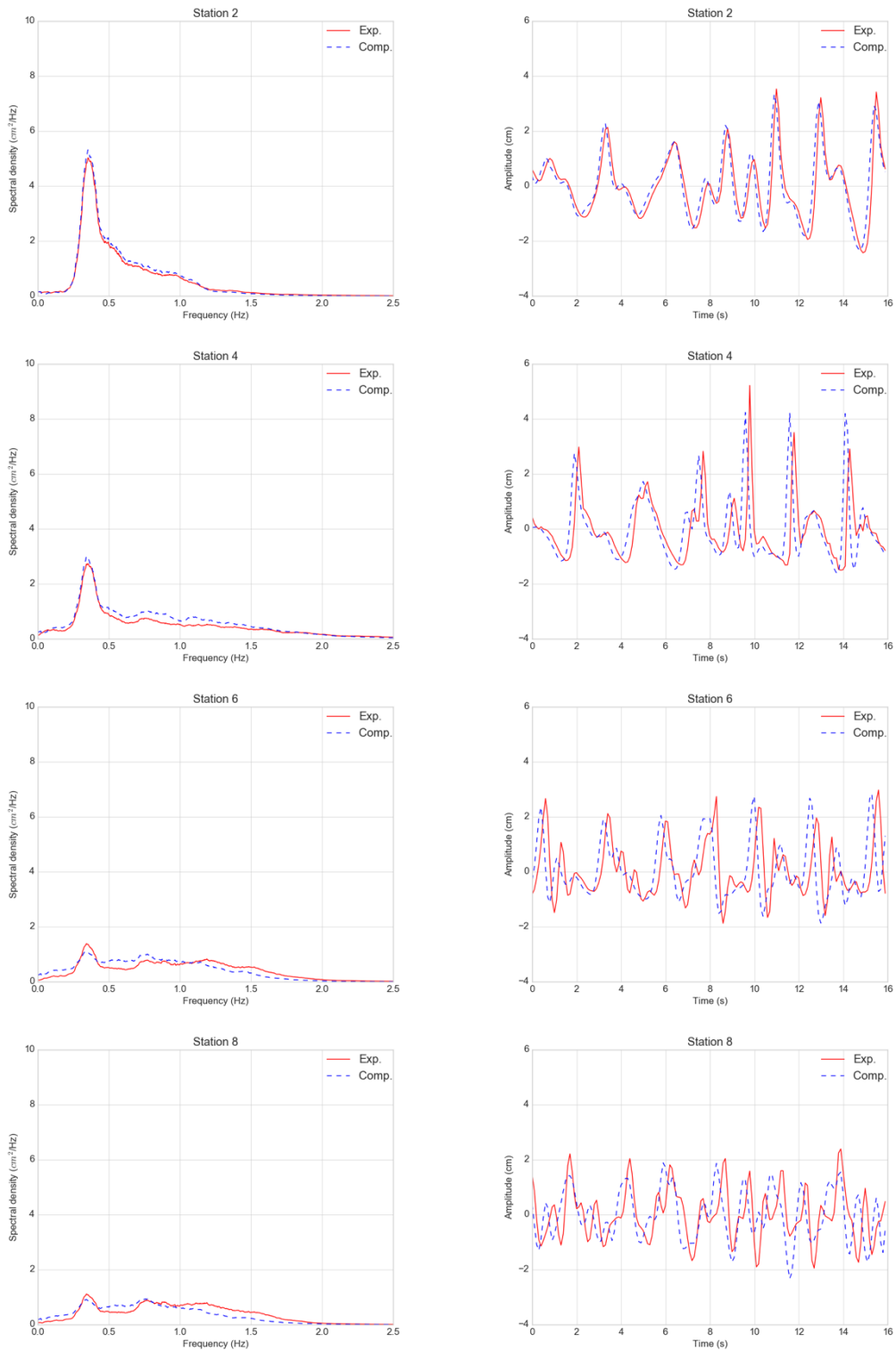


Figure 5. Random spilling-breaking long waves with  $f_p = 0.4 \text{ Hz}$  over a submerged bar. Left column shows wave spectra, right column shows time domain series. Solid line: experimental measurements, dashed line: computational results.



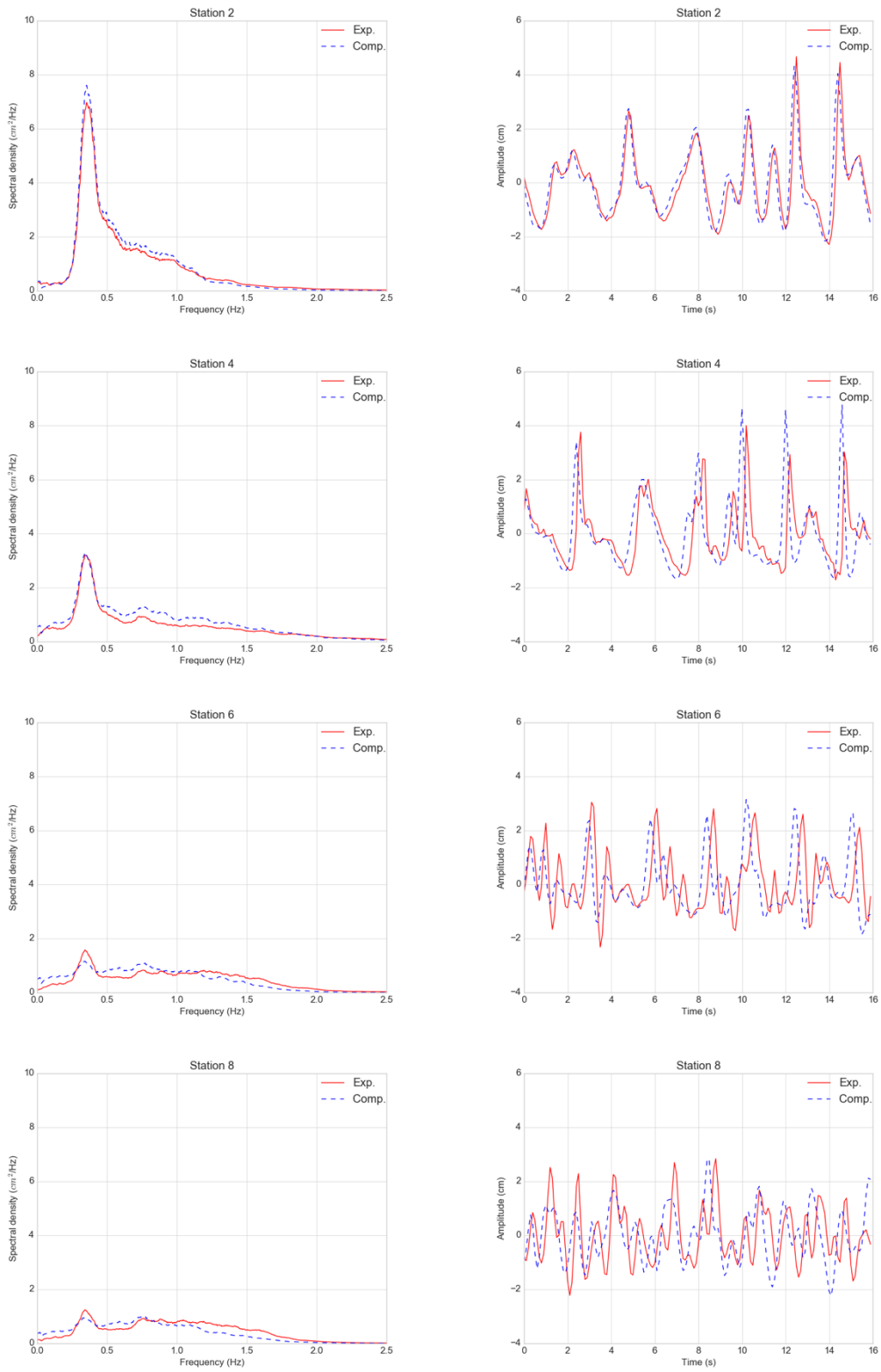


Figure 6. Random plunging-breaking long waves with  $f_p = 0.4$  Hz over a submerged bar. Left column shows wave spectra, right column shows time domain series. Solid line: experimental measurements, dashed line: computational results.

### Breaking waves in surf zone

Field measurements pose a more challenging case to simulate in comparison to laboratory experiments due to complexity of the wave field and the higher nonlinearity involved. Since station 7 served as the incoming boundary condition, it is not shown here. It should be remarked that bottom geometry was represented with some smoothing.

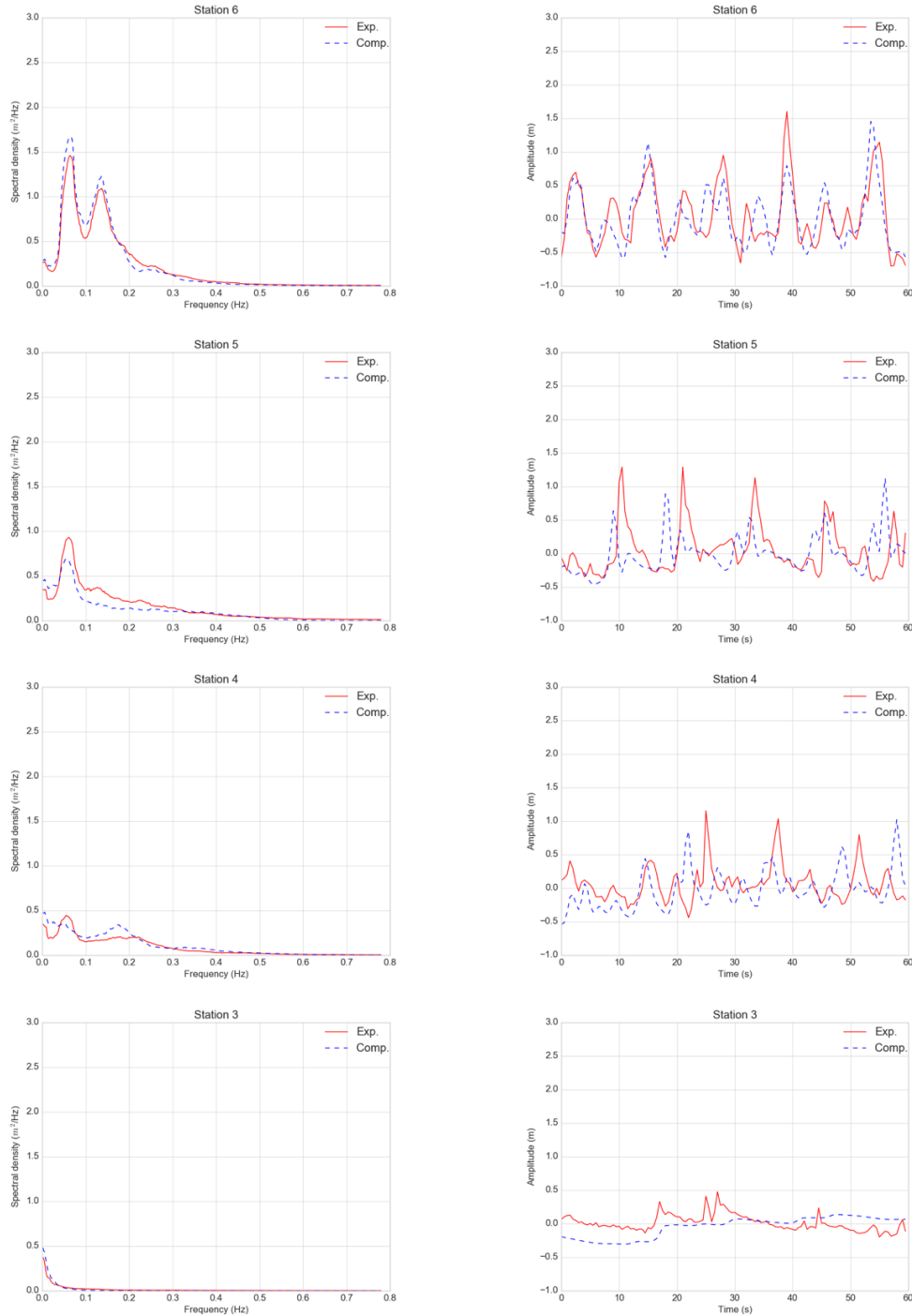


Figure 7. Breaking waves in the surf zone with  $f_p = 0.078125$  Hz at Station 6,5,4, and 3. Left column shows wave spectra, right column shows time domain series. Solid line: field measurements, dashed line: computational results.

The spectral results show acceptable agreement, especially if allowances are made for the uncertainties involved in the directionality of waves and the exact form of the bottom topography. However, results of the numerical simulations deviate towards the swash zone. A phase shift also exists here as in the simulations of laboratory experiments.

#### CONCLUSION

The spectral model of Beji and Nadaoka (1997), which is capable of simulating both non-breaking and breaking waves is used for the simulation of non-breaking and breaking waves in laboratory experiments and field measurements. The agreement is quite reasonable for spectral domain results. Although time domain results show acceptable agreement for the simulations of laboratory experiments, field measurement simulations deviate more.

Results suggest that the dissipation term should be modified in order for improving the predictions of the numerical model. Further, the phase shift problem must also be remedied.

#### REFERENCES

- Battjes, J. A. (1986) *Energy dissipation in breaking solitary and periodic waves*. Delft.
- Battjes, J. A. and Janssen, J. P. F. M. (1978) 'Energy Loss And Set-Up Due To Breaking Of Random Waves', in *Coastal Engineering*. Hamburg, Germany, pp. 569–587.
- Beji, S. and Battjes, J. A. (1993) 'Experimental investigation of wave propagation over a bar', *Coastal Engineering*, 19(April), pp. 151–162. doi: 10.1016/0378-3839(93)90022-Z.
- Beji, S. and Nadaoka, K. (1997) 'Spectral Modelling of Nonlinear Wave Shoaling and Breaking over Arbitrary Depths', in *Coastal Dynamics*, pp. 285–294.
- Beji, S. and Nadaoka, K. (1999) 'A spectral model for unidirectional nonlinear wave propagation over arbitrary depths', *Coastal Engineering*, pp. 1–16.
- Eldeberky, Y. and Battjes, J. A. (1996) 'Spectral modeling of wave breaking: Application to Boussinesq equation', *Journal of Geophysical Research*, 101(C1), pp. 1253–1264.
- Nakamura, S. and Katoh, K. (1992) 'Generation of Infragravity Waves in Breaking Process of Wave Groups', in *Coastal Engineering*. Venice, Italy, pp. 990–1003.
- Svendsen, I. A. (1984a) 'Mass flux and undertow in a surf zone', *Coastal Engineering*, 8(4), pp. 347–365. doi: [http://dx.doi.org/10.1016/0378-3839\(84\)90030-9](http://dx.doi.org/10.1016/0378-3839(84)90030-9).
- Svendsen, I. A. (1984b) 'Wave heights and set-up in a surf zone', *Coastal Engineering*, 8(4), pp. 303–329. doi: [http://dx.doi.org/10.1016/0378-3839\(84\)90028-0](http://dx.doi.org/10.1016/0378-3839(84)90028-0).
- Zelt, J. A. (1991) 'The run-up of nonbreaking and breaking solitary waves', *Coastal Engineering*, 15(3), pp. 205–246. doi: 10.1016/0378-3839(91)90003-Y.